

# Efficiency of the Equivalent Slab Thickness of the Ionosphere to Set Radio Wave Propagation Conditions

Olga Maltseva and Natalia Mozhaeva

*Institute for Physics, Southern Federal University, Stachki, 194, Rostov-on-Don, Russia*  
mal@ip.rsu.ru

**Keywords:** GPS, Total electron content TEC, Ionospheric models, Equivalent slab thickness.

**Abstract:** Now the total electron content TEC is a key parameter characterizing conditions of the ionosphere. TEC is widely used for an estimation of positioning accuracy, definition of index of ionospheric storm activity. Data of TEC is very important for systems of satellite communication and navigation. The advantages of the TEC measurement are the systems of a large number of receivers, the possibility of continuous global monitoring of the ionosphere, the availability of data on the Internet. For many systems (HF-communication, HFDF, HFGINT) it is necessary to know the maximum density of the ionosphere NmF2 or, that is equivalent, a critical frequency foF2. To obtain NmF2, it is necessary to know the proportionality coefficient  $\tau = \text{TEC}/\text{NmF2}$ , which is the equivalent slab thickness of the ionosphere. Before occurrence of navigational satellites, no special attention was given to this parameter and there were many inaccuracies in the papers devoted to  $\tau$ . The possibility of the global monitoring of NmF2 with use of TEC, measured by navigational satellites, makes to give the more close attention to its study. In the present paper, data of more than 50 ionospheric stations and several global maps of TEC are used to investigate behavior of a median  $\tau(\text{med})$  of the observational equivalent slab thickness  $\tau(\text{obs})$ . Comparison of  $\tau(\text{med})$  with the equivalent slab thickness  $\tau(\text{IRI})$  of the IRI model,  $\tau(\text{NGM})$  of the Neustrelitz global model and others has shown essential differences between these values. Approaches for developing a global model of  $\tau(\text{med})$  are offered. The most amazing are following results: (1) for a large amount of stations, the use of observational TEC and  $\tau(\text{IRI})$  worsens values of foF2 compared to the initial IRI model, (2) there are no fundamental quantitative differences in the use of  $\tau(\text{med})$  for all regions of the world, (3) the IRI model and maps of TEC (in the absence of GPS receivers) for the most northern Nord station (Greenland) showed surprisingly good agreement with the experimental values of foF2.

## 1 INTRODUCTION

The critical frequency of the ionosphere foF2 was the main parameter determining the state of the ionosphere and radio wave propagation conditions in the last century. It is connected with the maximum density NmF2 of the ionosphere by the relationship  $\text{NmF2} = 1.24_{10} \times \text{foF2}^2$  and with the maximum usable frequency MUF through the propagation factor M(D):  $\text{MUF} = \text{M(D)} \times \text{foF2}$ . This frequency is measured by ground ionosondes. In the 21st century, the total electron content TEC becomes the main parameter. TEC is measured by means of navigation satellites in units of  $\text{TECU} = 1_{10} 16 \text{ e/m}^2$ . The advantages of the TEC measurement are regional systems of a large number of receivers, the possibility of continuous global monitoring of the ionosphere, the availability of data on the Internet. Naturally,

there was a proposal to use TEC to determine the maximum density of the ionosphere NmF2 and foF2. To do this, we need to know the proportionality coefficient  $\tau = \text{TEC}/\text{NmF2}$ , which is the equivalent slab thickness of the ionosphere. Despite the fact that the measurement of NmF2 was begun with the invention of ionosondes (Breit and Tuve, 1926) and TEC measurements were begun with the first artificial satellite launch (Aitchison and Weekes, 1959), and the opportunity to use  $\tau$  to obtain knowledge of the ionosphere parameters and the atmosphere was immediately appreciated, interest in this parameter was increased only with the advent of satellite navigation systems GPS, GLONASS, allowing measurement of TEC. Despite the huge amount of publications, unified picture of the behavior of the experimental equivalent slab thickness  $\tau(\text{obs})$  does not exist because different data

is used to determine TEC. Distinctions concern both technical characteristics, and heights of satellites. Traditionally the International Reference Ionosphere model IRI (Bilitza, 2001; Bilitza et al., 2014) and its equivalent slab thickness  $\tau$ (IRI) are used to calculate foF2. However, on one hand,  $\tau$ (IRI) is not an empirical model in a statistical sense, but, on the other hand, almost nobody compared values of  $\tau$ (obs) and  $\tau$ (IRI) and suggested the use of experimental median  $\tau$ (med) to calculate foF2. In (Maltseva et al. 2011), it was proposed to use  $\tau$ (med) together with the experimental values TEC(obs) and it was shown that this use allows to obtain foF2 closer to the experimental value foF2(obs) than by means of  $\tau$ (IRI), and to fill gaps of the experimental data of foF2.

The aim of this article is to estimate: (1) the features of the behavior of the median equivalent slab thickness, (2) the effectiveness of its use together with the total electron content to obtain the critical frequencies in comparison with the equivalent slab thickness of current models of the ionosphere, (3) the opportunity of developing a global model of  $\tau$ (med).

## 2 EXPERIMENTAL DATA AND CALCULATED VALUES

The feature of the current stage of research is the availability of online databases of experimental data that allows us to obtain the results on a global scale (Maltseva, 2015). Data of foF2 of 56 ionosondes of vertical sounding were used together with 5 global maps JPL, CODE, UPC, ESA, IGS (Hernandez-Pajares et al., 2009). The disadvantage of ionospheric data is their sketchy character however there are stations for which long-term measurements are available. Data of foF2 was taken from the databases SPIDR (<http://spidr.ngdc.noaa.gov/spidr/index.jsp>) and DIDBase (<http://ulcar.uml.edu/DIDB/>). TEC values were calculated from IONEX files (<ftp://cddis.gsfc.nasa.gov/pub/gps/products/ionex/>). As models, we used IRI2001, IRI2012 (Bilitza, 2001; Bilitza et al., 2014), which have the upper limit of 2,000 km, and IRI-Plas (Gulyaeva, 2003; Gulyaeva and Bilitza, 2012) located on the site <http://ftp.izmiran.ru/pub/izmiran/SPIM/> and allowed determining N(h)-profile up to heights of navigation satellites h(GPS) by taking into account a plasmaspheric part of the profile. The magnitude of the equivalent slab thickness  $\tau$  is calculated in accordance with the relationship  $\tau = \text{TEC}/\text{NmF2}$  for the model and experimental parameters TEC and

NmF2. In this paper, values of  $\tau$ (IRI) of the IRI model and the median  $\tau$ (med) of observational  $\tau$ (obs) are calculated and compared. To evaluate the effectiveness of their use jointly with observational TEC(obs) we have introduced corresponding efficiency coefficients. These coefficients are determined by using the deviations of calculated foF2 from the observational foF2(obs). The value of  $|\Delta\text{foF2}(\text{IRI})| = |\text{foF2}(\text{obs}) - \text{foF2}(\text{IRI})|$  is the difference between the instantaneous values of the IRI model and observational foF2(obs). Monthly averages were calculated. This difference is in the denominators of the efficiency coefficients.  $|\Delta\text{foF2}(\tau(\text{IRI}))| = |\text{foF2}(\text{obs}) - \text{foF2}(\tau(\text{IRI}))|$  is the difference between the values calculated using  $\tau$ (IRI) and TEC(obs) and the observational foF2(obs). Deviation  $|\Delta\text{foF2}(\tau(\text{med}))| = |\text{foF2}(\text{obs}) - \text{foF2}(\tau(\text{med}))|$  is the difference between values calculated using  $\tau$ (med) and TEC(obs) and foF2(obs). Coefficient  $K_{\tau\text{IRI}} = |\text{foF2}(\Delta\text{IRI})| / |\Delta\text{foF2}(\tau(\text{IRI}))|$  is the coefficient of efficiency of joint use of  $\tau$ (IRI) and TEC(obs). Coefficient  $K_{\text{eff}} = |\Delta\text{foF2}(\text{IRI})| / |\Delta\text{foF2}(\tau(\text{med}))|$  is the coefficient of efficiency of joint use of  $\tau$ (med) and TEC(obs). These coefficients are given together with the line  $K = 1$  to visually evaluate the effectiveness of using TEC(obs): if the coefficient is 1, this means that the use of TEC(obs) leads to the same results of foF2, as the initial IRI model without TEC(obs). In this case  $|\Delta\text{foF2}(\text{IRI})| = |\Delta\text{foF2}(\tau(\text{IRI}))|$ . If the coefficient  $> 1$ , then the use of TEC(obs) leads to results better than the initial model. If the coefficient is higher than 1, then the use of TEC(obs) worsens the results of the model. These values determine how strongly the deviation of the initial model differs from the deviation of values calculated using  $\tau$ (IRI) and  $\tau$ (med) together with TEC(obs).

## 3 FEATURES OF $\tau$ BEHAVIOR

In the literature, there are certain disagreements in the describing of such features of  $\tau$  as: 1) diurnal variation, 2) seasonal variation, 3) latitudinal dependence 4) dependence on solar activity, 5) behavior during disturbed conditions. The most important disagreement is the absence or weakness of the latitudinal dependence of  $\tau$ , noted in many publications (Kouris et al., 2008; Sardar et al., 2012; Vryonides et al., 2012). Real situation is given in Figure 1.

If the latitudinal dependence of  $\tau$ (med) was absent, the value of  $\tau$ (med) for one station could be used in obtaining foF2 with the observational TEC in

the whole region. Of particular importance is the study of the behavior of  $\tau(\text{obs})$  during disturbances because it is different from the behavior of  $\tau(\text{med})$ . In paper (Maltseva et al. 2011), a hyperbolic approximation of  $\tau$  was introduced as  $\tau(\text{hyp}) = b_0 + B1/Nm$  to build a regression relation in which  $Nm = foF2 * foF2$  ( $foF2$  in MHz). Such function is calculated for each map. An example is shown in Figure 2. Approximation of  $\tau(\text{hyp})$  was built for a more accurate determination of  $\tau$  during the disturbances.

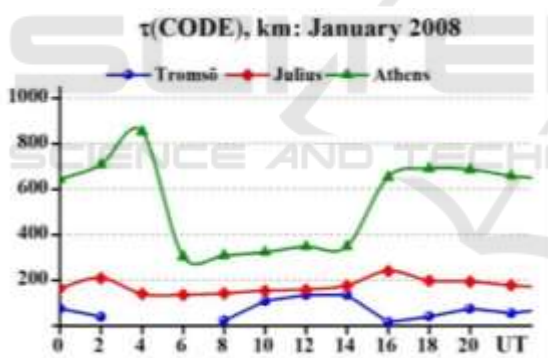
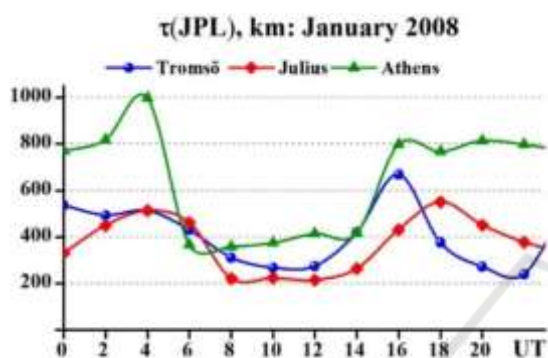


Figure 1. Example of the diurnal variation of  $\tau(\text{obs})$  for the different latitude and two maps JPL and CODE.

The most important is the difference between  $\tau(\text{IRI})$  and  $\tau(\text{med})$ . Numerous examples are given in papers (Maltseva and Mozhaeva, 2014, 2015) for stations in all regions of the world with long-term data. Example for the etalon station Juliusruh is shown in Figure 3.

Large difference is seen not only in magnitude but also in the diurnal variation. Namely this difference determines the difference of the critical frequency  $foF2(\text{rec})$  reconstructed from the observational values  $\text{TEC}(\text{obs})$  using  $\tau(\text{med})$  and  $\tau(\text{IRI})$ .

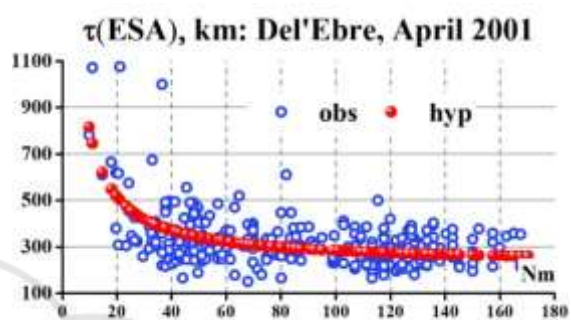
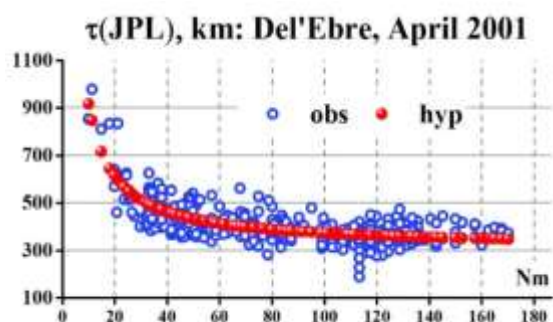


Figure 2: An example of a hyperbolic dependence of  $\tau$  for the disturbed month.

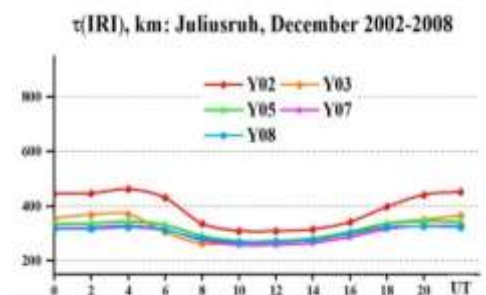
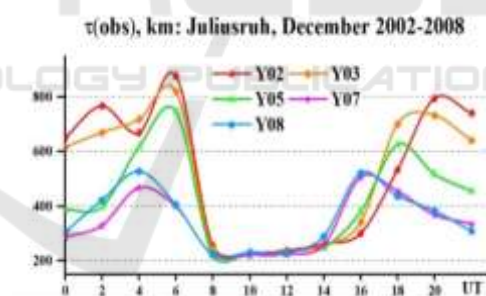


Figure 3: Differences of the model and the experimental equivalent slab thicknesses in the example for the mid-latitude station Juliusruh of European region and JPL map.



#### 4 EFFICIENCY OF JOINT USING $\tau$ (IRI) AND $\tau$ (MED) AND TEC(OBS)

Figure 4 shows the deviation of the calculated values of foF2 from foF2(obs) and efficiency coefficients for stations with long-term observations: high- latitude

Thule, mid-latitude Juliusruh and equatorial Kwajalein stations of the northern hemisphere and the high-latitude Mawson station of the southern hemisphere. Black dots show the results for the IRI model, triangles present the results of joint using  $\tau$ (IRI) and TEC(obs), circles give the results of joint using  $\tau$ (med) and TEC(obs).

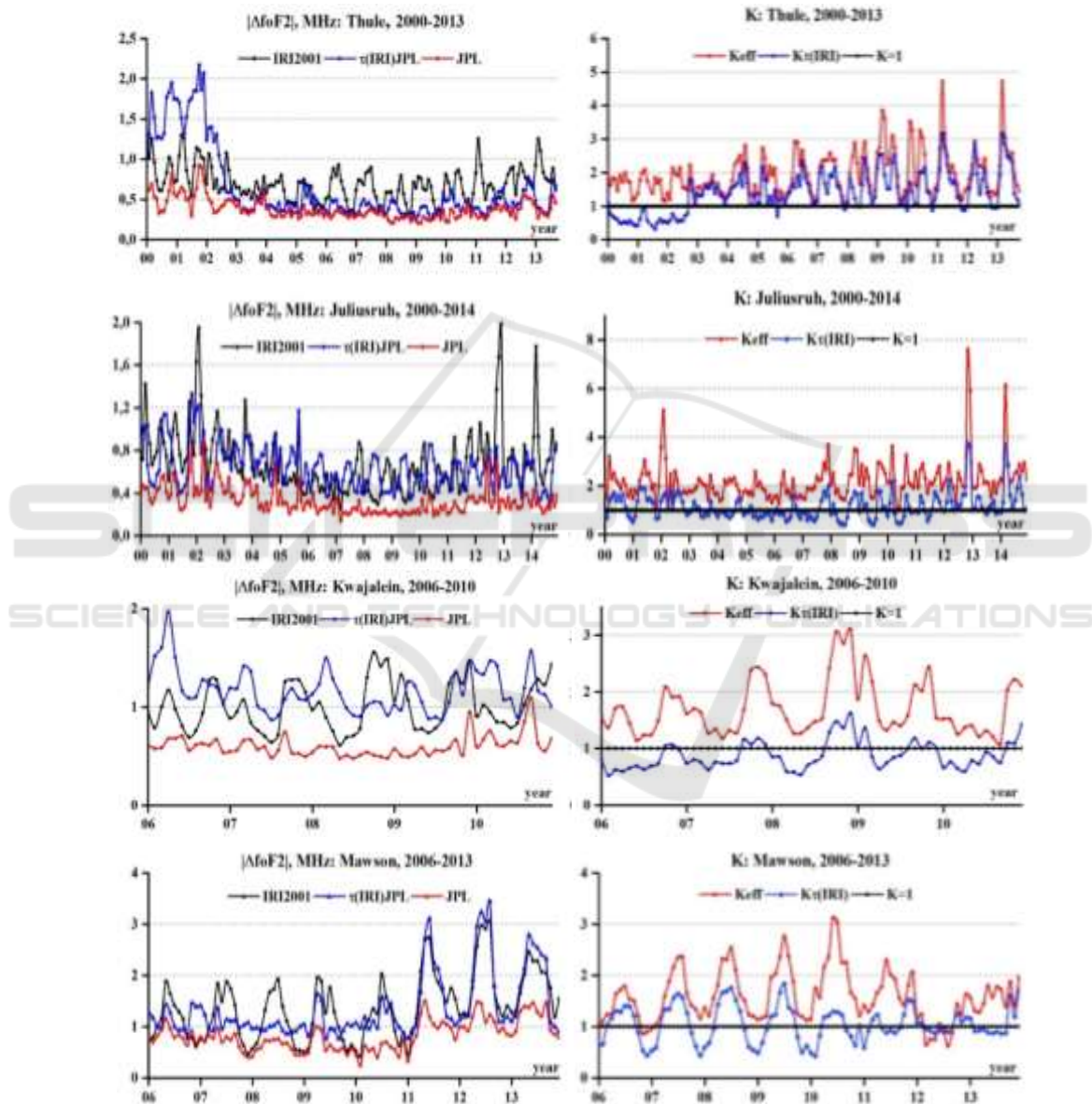


Figure 4: Deviations  $|\Delta foF2|$  and efficiency coefficients for the IRI model and two cases of using  $\tau$ (IRI) and  $\tau$ (med) together with the TEC(obs).

It can be seen that the joint use of  $\tau$ (IRI) and TEC(obs) ( $K < 1$ ) can significantly worsen the

calculation of foF2 compared with the model ( $K < 1$ ). By using  $\tau$ (med) and TEC(obs) deviations  $|\Delta foF2|$  do

not exceed 1.0 MHz in most cases even in problematic areas, such as high and equatorial latitudes, and the coefficients are always exceed 1. In the previous 2-3 years, a large amount of ionospheric data has become available. This allows us to check and compare the results simultaneously on many stations on a global scale, in particular, to obtain these results in the points in which they have not been obtained and the IRI model was not tested itself. We selected April 2014 and March 2015, because they included geomagnetic disturbances.

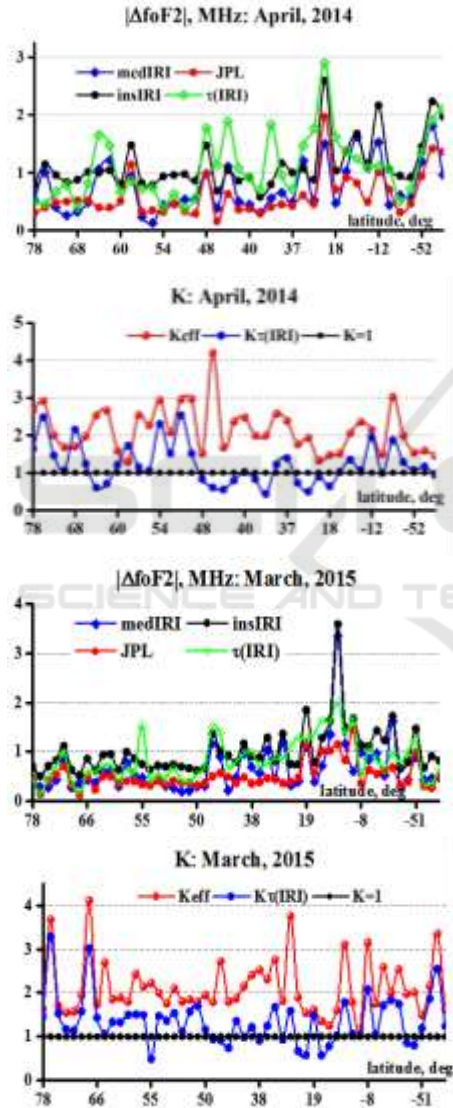


Figure 5: Correspondence between the model and the observational values of foF2 and efficiency coefficients on a global scale in April 2014 and March 2015.

Figure 5 illustrates the effectiveness of using  $\tau(\text{med})$  globally by example of data for April 2014 (minimum Dst = -81 nT) and March 2015 (minimum

Dst = -223 nT). The samples shown on the x axis are with a variable step, as stations are located not uniformly.

It is evident that in the northern hemisphere the amount of stations is larger than in the southern one. In all cases, the use of  $\tau(\text{med})$  and TEC(obs) improves matching calculated foF2(rec) with foF2(obs) compared with two options: using the initial IRI model and joint using  $\tau(\text{IRI})$  and TEC(obs). Joint using  $\tau(\text{IRI})$  and TEC(obs) may provide poor results compared to the initial model. The best results were obtained for mid-latitudes. For high latitudes they were not worse, but in the equatorial latitudes problems for the model are seen, although the joint use of  $\tau(\text{med})$  and TEC(obs) mitigates these problems. Figure 6 gives the results for the Nord station (Greenland) which are of particular interest because it is the most northern station. Unfortunately data of this station in the DIDbase were downloaded recently and in a very limited extent (a few months and not each year).

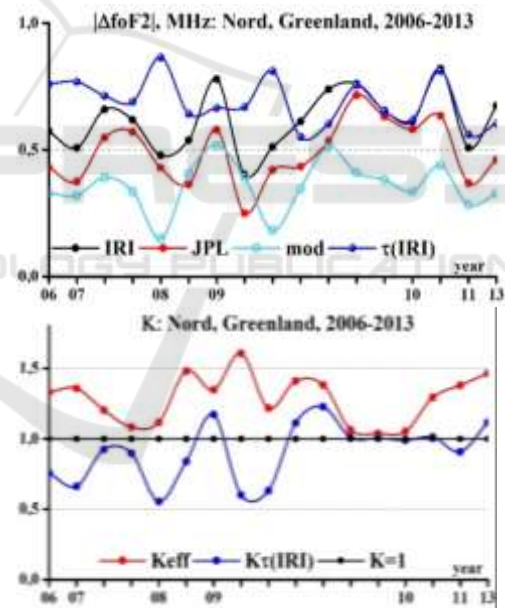


Figure 6: Long-term statistics for the Nord station (Greenland) for available months of years indicated on the x axis.

The results are almost similar to the results for Thule, Tromso and other lower high-latitudinal stations. Since the critical frequency of the Nord station has never been compared with the model the upper-hand plot of Figure 6 presents the curve showing the deviation of the model from the experimental medians of foF2. Results indicate a surprisingly good performance of the IRI model in this region.

## 5 ABOUT THE CONSTRUCTION OF A GLOBAL MODEL OF $\tau(\text{MED})$

The mention of the opportunity to construct a model of  $\tau$  is practically absent in the papers, but in recent years some articles were published on the use of TEC and the ionospheric equivalent slab thickness  $\tau$  to determine NmF2, what confirms the importance of this problem. In (Gerzen et al., 2013), the authors have proposed the use of two Neustrelitz models of TEC and NmF2 (Hoque and Jakowski, 2011; Jakowski et al., 2011) for the calculation of foF2, but without sufficient testing. We use these models under one name NGM (from Neustrelitz Global Model). It is obvious that authors of (Gerzen et al., 2013) have also used the value of  $\tau(\text{NGM}) = \text{TEC}(\text{NGM})/\text{NmF2}$ , which can serve as an empirical model of  $\tau$ . However, testing this model in (Maltseva et al., 2013, 2014) showed that in many regions the value of  $\tau(\text{NGM})$  is very different from the experimental  $\tau(\text{med})$ . In (Muslim et al., 2015), a model of the average values of  $\tau$  was proposed as expansion in Fourier series according to the TEC of the global map CODE and foF2 for 21 stations, however, the assumptions made in constructing the model: (1) linear dependence of all parameters of the TEC, foF2 and  $\tau$  on solar activity, (2) lack of longitudinal dependence of these parameters at the same local time LT, (3) regularity of  $\tau$  in quiet and disturbed conditions need confirmation. This allows drawing a conclusion about the need to develop the model of  $\tau$ . To build a model of  $\tau(\text{med})$  on a global scale two approaches are proposed: two-parameter model based on a hyperbolic approximation  $\tau(\text{hyp}) = b_0 + b_1/\text{NmF2}$  and the use of the coefficient  $K(\tau) = \tau(\text{med})/\tau(\text{IRI})$ , since the construction of the model using the values themselves is not possible because of the large variability of values (in particular, the pre-sunrise peak on some latitudes). A hyperbolic dependence and approximation coefficient  $K(\tau)$  were calculated for March 2015. The results are shown for two regions 2 ( $15^\circ\text{E} < \lambda < 40^\circ\text{E}$ ) with 8 stations and 4 ( $110^\circ\text{E} < \lambda < 170^\circ\text{E}$ ) with 9 stations and two wider zones (Lat1 and Lat2). Area Lat1 includes stations, located mostly in American continent of northern and southern hemispheres. Area Lat2 includes stations from European, Siberian and South-Eastern regions. Behavior of coefficients  $b_0$  and  $b_1$  is shown in Figure 7 for these regions.

The test results of this model are shown in Table 1

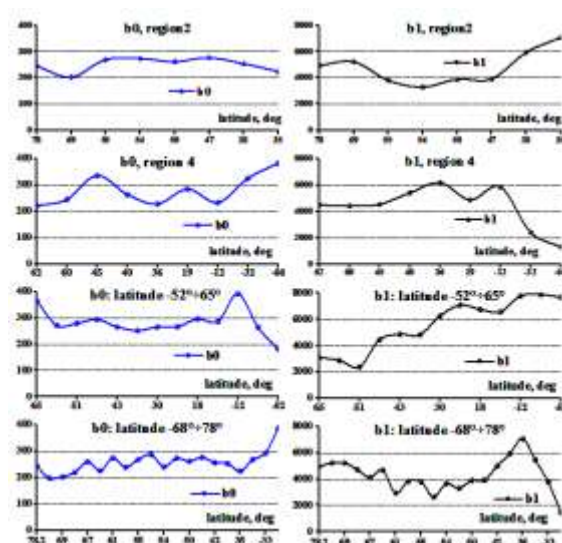


Figure 7: Behavior of hyperbolic approximation coefficients in various regions

Table 1 includes different deviations. Column 1 indicates the station name and the region to which it belongs. The second column shows the coefficients of the hyperbolic approximation of  $\tau(\text{obs})$  for the corresponding station. The third column specifies conditions to which the two rows of values belong. The top line (full) indicates average for all days of the month, the bottom line (dist) gives average for disturbed days (from 16 to 21 March). The fourth column shows the results for the initial IRI model, the fifth column presents the absolute difference between the foF2(obs) and the values calculated using  $\tau(\text{med})$  and TEC(obs). Column 6 contains the frequency deviation, calculated using the coefficients  $b_0$  and  $b_1$  of the hyperbolic approximation for a given station. The remaining columns give results of using coefficients of areas referred to in the line title. All of these values should be compared with the values for the IRI model in bold. This is a test of the effectiveness of the model. It can be seen that all values are higher in disturbed days and the largest differences concern to the initial IRI model. It is seen that frequencies of one region could be used to calculate the coefficients for other region. This demonstrates a global character of the model of  $\tau(\text{med})$ .

Another method of constructing a global model of  $\tau(\text{med})$  would be to use the coefficients  $K(\tau) = \tau(\text{med})/\tau(\text{IRI})$ . Definite advantage of this model might be in the fact that its denominator is the value of  $\tau(\text{IRI})$ , which has a global character, and a small change in  $K(\tau)$  in areas with close latitudes.

The distinction is development of a model for each hour. The degree of proximity of  $\tau$  is better

illustrated in the circular diagram. An example of some diagrams is shown in Figure 8 for region 4 for UT = 0, 6, 12, and 18 on March 2015. The red line shows the value of coefficient  $K(\tau)$ , green triangles

are the average values, the blue quadrates concern circles with radius  $R = 1$ .

Table 1: Deviation of frequencies, calculated by the hyperbolic dependence, from the experimental values in March 2015.

1	2	3	4	5	6	7	8	9	10
station	b1, b0		IRI	rec	stat	reg2	reg4	Lat1	Lat2
Juliusruh	3295.5	full	<b>0.73</b>	0.41	0.43	0.68	0.67	1.03	0.57
reg2	273.2	dist	<b>1.44</b>	0.52	0.49	0.67	0.68	1.07	0.64
Athens	5929.3	full	<b>0.91</b>	0.36	0.46	0.56	0.48	0.52	0.58
reg2	253.2	dist	<b>1.31</b>	0.44	0.74	0.52	0.59	0.87	0.51
Grahamstown	3788.7	full	<b>0.80</b>	0.40	0.54	0.77	0.59	0.73	0.73
Lat2	293.2	dist	<b>1.54</b>	0.46	0.62	0.84	0.75	0.82	0.77
Longyearbyen	4947.1	full	<b>0.70</b>	0.43	0.62	0.60	0.58	0.82	0.58
Lat2	244.2	dist	<b>0.69</b>	0.49	0.73	0.69	0.69	1.01	0.63
Thule	692.7	full	<b>0.51</b>	0.14	0.15	0.56	0.42	0.47	0.59
	437.6	dist	<b>0.55</b>	0.10	0.13	0.51	0.46	0.64	0.54
Millstonehill	4864.4	full	<b>0.90</b>	0.50	0.47	0.48	0.46	0.67	0.49
Lat1	265.4	dist	<b>1.38</b>	0.67	0.67	0.65	0.81	0.81	0.80
Bejing	5402.8	full	<b>1.17</b>	0.49	0.61	0.61	0.58	0.70	0.62
reg4	263.9	dist	<b>1.99</b>	0.42	0.64	0.45	0.51	0.84	0.45
Kokubunji	6176.7	full	<b>1.29</b>	0.47	0.65	0.61	0.69	0.85	0.62
reg4	228.4	dist	<b>2.11</b>	0.55	0.66	0.56	0.70	0.96	0.56
Niue Island	4874.7	full	<b>1.85</b>	1.15	1.36	1.35	1.28	1.43	1.29
reg4	285.0	dist	<b>1.67</b>	0.71	1.00	0.73	0.85	1.11	0.67
Cocos Island	5467.3	full	<b>1.43</b>	0.55	0.68	0.86	0.62	0.65	0.82
Lat2	267.8	dist	<b>1.66</b>	0.52	0.77	0.88	0.67	0.80	0.83
Mawson	1466.2	full	<b>0.91</b>	0.27	0.37	1.00	0.85	1.02	0.92
Lat2	386.8	dist	<b>1.12</b>	0.12	0.21	0.80	0.98	0.98	0.81



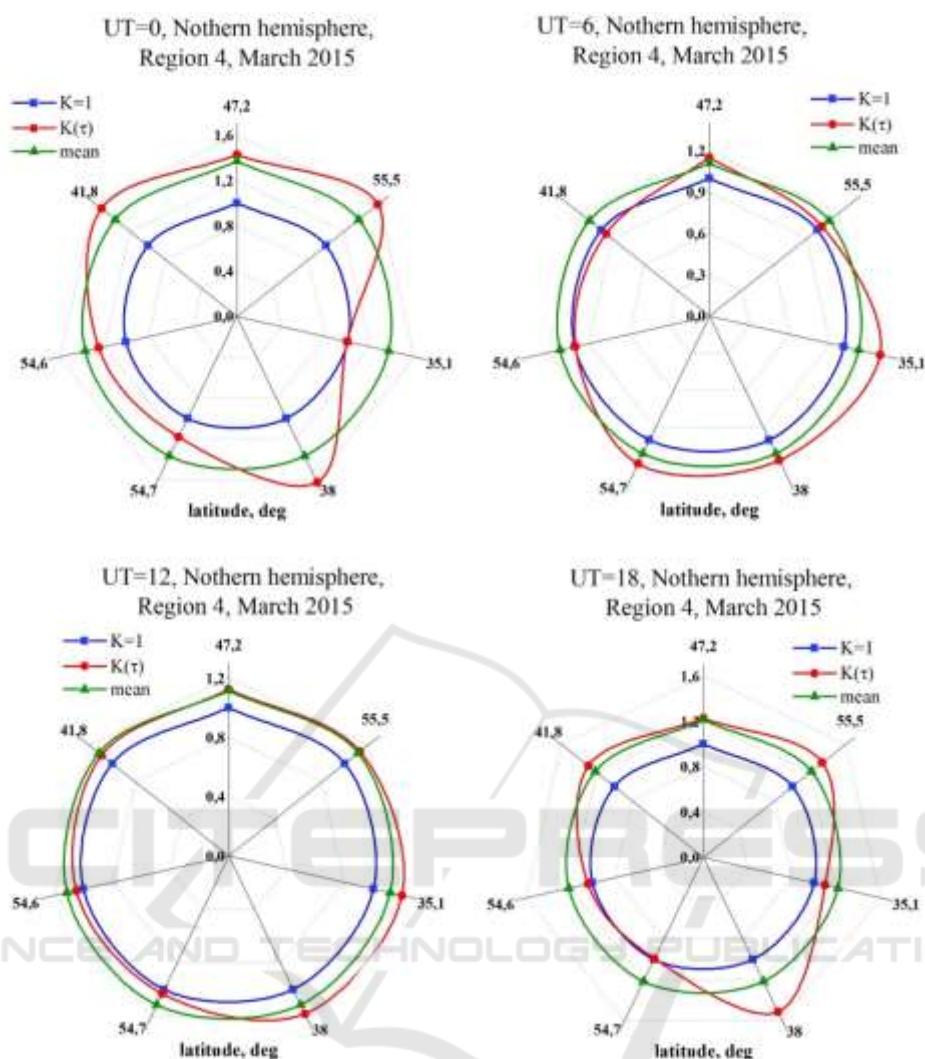


Figure 8: Illustration of charts for the coefficient  $K(\tau)$ .

The model is the average value  $K(\text{mean})$ . The algorithm of its use is calculation of the new value  $\tau(K\tau) = K(\text{mean}) \times \tau(\text{IRI})$  and the use of this new value together with  $\text{TEC}(\text{obs})$  to calculate foF2. To test the efficiency of the algorithm, averages of  $K(\text{mean})$  were calculated for 7 stations for region consisted of 8 stations and were used to calculate foF2 for the 8<sup>th</sup> station. Results are presented in Figure 9 as deviations of the calculated values from observational foF2(obs) for the four stations: Pruhonice, Gorkovskaya, Tunguska and Ramey.

Table 2. Average deviations of calculated foF2 from foF2(obs) using various options of models and  $\tau$ .

station	IRI-off	IRI-on	$\tau(\text{IRI})$	new	$\tau(\text{med})$
Pruhonice	0.63	0.65	0.54	0.34	0.32
Gorkovsk	0.64	0.60	0.43	0.37	0.36
Tunguska	0.95	0.86	0.72	0.57	0.50
Ramey	0.78	0.85	1.36	0.78	0.58



All plots contain curves of deviations for the initial model without the use of TEC. Since both options (off and on) were used, the curves were indicated by IRI-off and IRI-on. Curves with the icon  $\tau$ (IRI) show results of joint using of  $\tau$ (IRI) and TEC(obs).

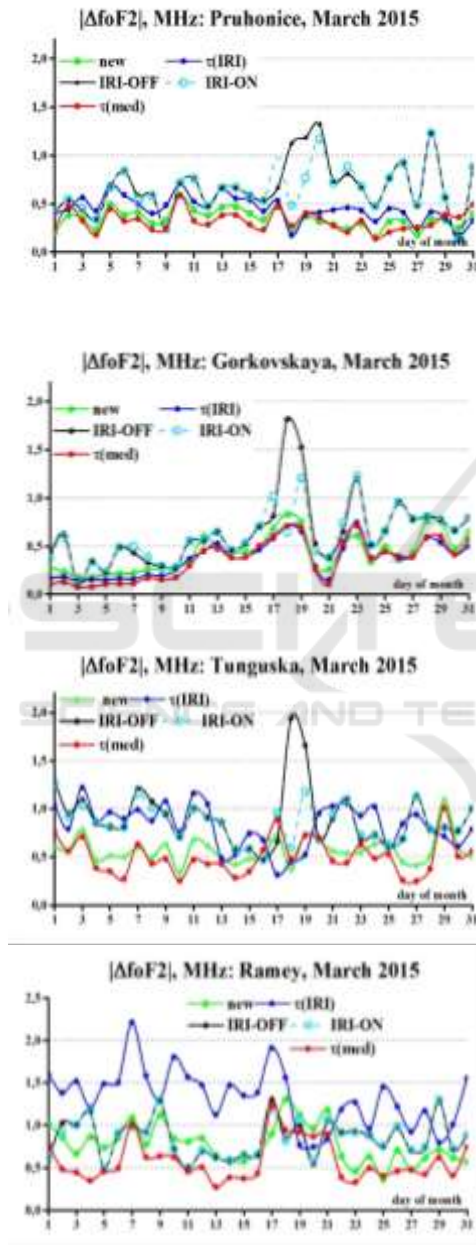


Figure 9: Deviation of calculated foF2 values from foF2(obs) using various options of  $\tau$ .

The curves marked by “new” show test values for the  $K\tau$  model. Asterisks present results for  $\tau$ (med) and TEC(obs). Most values of  $|\Delta\text{foF2}|$  do not exceed 1

MHz. Significant deviations are only visible to the IRI model in disturbed days on March 18-21 for the case  $\tau$ (IRI) and for the Ramey station. Quantitative characteristics are given in Table. 2.

## 6 CONCLUSIONS

Data of more than 50 ionospheric stations and several global maps of TEC were used to study behavior of a median  $\tau$ (med) of the observational equivalent slab thickness  $\tau$ (obs) and comparisons with existing models  $\tau$ (IRI),  $\tau$ (NGM) and others. Essential differences between them, leading to the large deviations of the calculated values of foF2 from the experimental ones are shown. As a quantitative estimation, the effectiveness coefficients of joint using TEC(obs) and  $\tau$ (med) in comparison with joint using TEC(obs) and  $\tau$ (IRI) are used. It is shown that the effectiveness coefficients practically always exceed 1 for joint using of TEC(obs) and  $\tau$ (med). There are several striking results: (1) for a large amount of stations, the use of observational TEC and  $\tau$ (IRI) worsens values of foF2 compared to the initial IRI model, (2) there are no fundamental quantitative differences in the use of  $\tau$ (med) for all regions of the world, (3) the IRI model and maps of TEC (in the absence of GPS receivers) for the most northern Nord station (Greenland) showed surprisingly good agreement with the experimental values of foF2. In this sense, results of HF propagation modeling on high-latitude paths based on the IRI model (Blagoveshchensky et al., 2016) seem no longer surprising. Two approaches for developing a global model of  $\tau$ (med) are offered.

## ACKNOWLEDGEMENTS

The authors thank the scientists who provided data of SPIDR and DIDBase, global maps of TEC, operation and modification of the IRI model, Southern Federal University for financial support (grant N 213.01-11/2014-22).

## REFERENCES

Aitchison, G.J., Weekes, K., 1959. Some deductions of ionospheric information from the observations of emissions from satellite 1957a2—I: The theory of the analysis, *J. Atm. Terr. Phys.*, 14(3–4), 236–243. doi:10.1016/0021-9169(59)90035-2.

- Bilitza, D., 2001. International Reference Ionosphere, *Radio Sci.*, 36(2), 261-275.
- Bilitza, D., Altadill, D., Zhang, Y., Mertens, C., Truhlik, V., Richards, P., McKinnell, L.-A., Reinisch, B., 2014. The International Reference Ionosphere 2012 – a model of international collaboration, *J. Space Weather Space Clim.*, 4, A07, 12p. DOI: 10.1051/swsc/2014004.
- Blagoveshchensky, D.V., Maltseva, O.A., Anishin, M.M., Rogov, D.D., Sergeeva, M.A., 2016. Modeling of HF propagation at high latitudes on the basis of IRI, *Adv. Space Res.*, 57, 821–834.
- Breit, G., Tuve, M.A., 1926. A test for the existence of the conducting layer, *Phys. Rev.*, 28, 554-575.
- Gerzen, T., Jakowski, N., Wilken, V., Hoque, M.M., 2013. Reconstruction of F2 layer peak electron density based on operational vertical total electron content maps, *Ann. Geophys.*, 31, 1241-1249. doi:10.5194/angeo-31-1241-2013.
- Gulyaeva, T.L., 2003. International standard model of the Earth's ionosphere and plasmasphere, *Astron. and Astrophys. Transaction*, 22, 639-643.
- Gulyaeva, T., Bilitza, D., 2012. Towards ISO Standard Earth Ionosphere and Plasmasphere Model, In: *New Developments in the Standard Model*, (R.J. Larsen ed.). NOVA, Hauppauge, New York, 1–48.
- Hernandez-Pajares, M., Juan, J. M., Orus, R., Garcia-Rigo, A., Feltens J., Komjathy, A., Schaer, S.C., Krankowski, A. 2009. The IGS VTEC maps: a reliable source of ionospheric information since 1998, *J. Geod.*, 83, 263–275.
- Hoque, M.M., Jakowski, N., 2011. A new global empirical NmF2 model for operational use in radio systems. *Radio Sci.*, 46, RS6015, 1-13.
- Jakowski, N., Hoque M.M., Mayer C., 2011. A new global TEC model for estimating transionospheric radio wave propagation errors, *J. Geod.*, 85(12), 965-974.
- Kouris, S.S., Polimeris, K.V., Cander, L.R., Ciraolo L., 2008. Solar and latitude dependence of TEC and SLAB thickness, *J. Atmos. Solar-Terr. Phys.*, 70, 1351-1365.
- Maltseva, O.A., 2015. Usage of the Internet resources for research of the ionosphere and the determination of radio-wave propagation conditions. *Proceedings of the Fourth International Conference on Telecommunications and Remote Sensing, Rhodes, Greece, 17-18 September, 7-17.*
- Maltseva, O.A., Mozhaeva, N.S., 2014. Features of behavior and usage of a total electron content in the Indian region, *International Journal of Engineering and Innovative Technology*, 4(4), October 2014, 1-9. www.ijet.com, ISSN: 2277-3754.
- Maltseva, O.A., Mozhaeva, N.S., 2015. Obtaining Ionospheric Conditions according to Data of Navigation Satellites, *International Journal of Antennas and Propagation*. 1-16. <http://dx.doi.org/10.1155/2015/804791>.
- Maltseva, O.A., Mozhaeva, N.S., Glebova, G.M., 2011. Global maps of TEC and conditions of radio wave propagation in the Mediterranean area, *PIERS Proceedings, Marrakesh, MOROCCO, March 20-23, 1P9\_0422, 1-5.*
- Maltseva, O.A., Mozhaeva, N.S., Nikitenko, T.V., 2014. Validation of the Neustrelitz Global Model according to the low latitude *Adv. Space Res.*, 54 () 463–472.
- Maltseva, O.A., Mozhaeva, N.S., Nikitenko T.V., 2015. Comparative analysis of two new empirical models IRI-Plas and NGM (the Neustrelitz Global Model), *Adv. Space Res.*, 55, 2086–2098.
- Maltseva, O., Mozhaeva, N., Vinnik, E., 2013. Validation of two new empirical ionospheric models IRI-Plas and NGM describing conditions of radio wave propagation in space. *Proceedings of Second International Conference on Telecommunications and Remote Sensing, Noordwijkerhout, The Netherlands, 11-12 July, 109-118.*
- Muslim, B., Haralambous, H., Oikonomou, Ch., Anggarani, S., 2015. Evaluation of a global model of ionospheric slab thickness for foF2 estimation during geomagnetic storm. *Ann. Geophys.*, 58(5), A0551. doi:10.4401/ag-6721.
- Sardar, N., Singh, A.K., Nagar, A., Mishra, S.D., Vijay, S.K., 2012. Study of Latitudinal variation of Ionospheric parameters - A Detailed report, *J. Ind. Geophys. Union*, 16(3), 113-133.